

УДК 528.21/22

## PARCULARITY OF THE GEOID DETERMINATION AT THE ANTARCTIC REGION

D.O. Marchenko, V.U. Maksymchuk

*Carpathian branch of the Subbotine Institute of Geophysics NAS Ukraine, Lviv, Naukova 3B Str.,  
dmitriy.marchenko@gmail.com*

**Summary.** The gravitation effect of topographic masses is very important for the gravity anomaly calculations and geoid heights determination. The new approach for the computation of the topographic-isostatic corrections and indirect effect of topography in spherical approximation is developed and tested in Antarctic region.

**Key words:** gravity, terrain effect, Moho, density, topographic-isostatic corrections.

**Реферат.** При вивченні гравітаційного поля Землі у випадку обчислення як гравітаційних аномалій, так і висот геоїда повинен бути врахований гравітаційний ефект топографічних мас. Розроблено методику обчислення топографо-ізоостатичних поправок та поправок на рельєф у сферичній апроксимації з перемінною густиною.

**Ключові слова:** сила тяжіння, територіальний ефект, Мохо, топографо-ізоостатичні поправки.

**Реферат.** При изучении гравитационного поля Земли в тех случаях, когда вычисляются как гравитационные аномалии, так и высоты геоида, следует учитывать гравитационный эффект топографических масс. Разработана методика вычисления топографо-изостатических поправок и поправок на рельеф в сферической аппроксимации с переменной плотностью.

**Ключевые слова:** сила притяжения, территориальный эффект, Мохо, топографо-изостатические поправки.

### Introduction

Computation of topographic corrections to measured values of functionals of the disturbing potential is one among key problems of the physical geodesy. In the frame of the classical approach to the determination of the disturbing potential based on the famous Stokes integral formula, introducing of such corrections provides the basic condition of absence of attracting masses outside the geoid. In the frames of advanced approaches based on application of the remove-restore procedure, introducing of topographic corrections leads to essential smoothing of a residual field due to elimination of very high frequencies. As a result, we may hope on more stable determination of the disturbing potential.

In general, the fundamental requirement of absence of zero-degree harmonic in the disturbing potential (Heiskanen and Moritz, 1967; Moritz, 1980; Neyman, 1979) can be violated by application of topographic mass potential  $V_T$  in the remove-restore procedure. This essential disadvantage may be eliminated by additional introducing the isostatic compensation potential  $V_I$  in accordance with one of known compensation model based on equal mass principle (Moritz, 1990). As a result, we come to the topographic / isostatic correction

$$V_{TI} = V_T + V_I. \quad (1)$$

At arbitrary point  $P$  at the Earth's surface the potential of masses located between the geoid surface

$$r_1 = r_1(\vartheta, \lambda), \quad (2)$$

and the Earth's physical surface

$$r_2 = r_2(\vartheta, \lambda), \quad (3)$$

may be defined by the integral (Heiskanen and Moritz, 1967):

$$V_T(P) = G \int_0^{2\pi} \int_{r_1}^{r_2} \int_0^{\vartheta} \rho_c \frac{r^2 \sin \vartheta}{l} dr d\vartheta d\lambda, \quad (4)$$

where, in general, the density  $\rho_c$  of the Earth's crust is considered as

$$\rho_c = \rho_c(r, \vartheta, \lambda). \quad (5)$$

In the above expressions  $G$  is the gravitational constant,  $l$  is spatial distance between the point  $P$  and the mass element  $dm = \rho_c r^2 \sin \vartheta dr d\vartheta d\lambda$ :

$$l = \sqrt{r_p^2 + r^2 - 2r_p r \cos \psi}, \quad (6)$$

$r_p$  is the geocentric distance of the point  $P$ ,  $\psi$  is the geocentric angular distance between the point  $P$  and the mass element  $dm$ :

$$\cos \psi = \cos \vartheta \cos \vartheta_p + \sin \vartheta \sin \vartheta_p \cos(\lambda - \lambda_p), \quad (7)$$

$\vartheta_p, \lambda_p$  are spherical coordinates (polar angle and longitude, respectively) of the point  $P$ , and  $\vartheta, \lambda$  are spherical coordinates of the mass element  $dm$ .

The potential of compensating masses located between the surfaces

$$t_1 = t_1(\vartheta, \lambda), \quad t_2 = t_2(\vartheta, \lambda), \quad (8)$$

may be defined in similar way by the integral

$$V_I(P) = G \int_0^{2\pi} \int_{t_1}^{t_2} \int_0^{\vartheta} \Delta \rho \frac{r^2 \sin \vartheta}{l} dr d\vartheta d\lambda, \quad (9)$$

with a variable density

$$\Delta \rho = \Delta \rho(r, \vartheta, \lambda). \quad (10)$$

With the definitions (4) and (9), total topographic / isostatic correction is expressed by the sum

$$V_{TI}(P) = V_T(P) + V_I(P), \quad (11)$$

and any linear geodetic functional (Moritz, 1980; Neyman, 1979) of the potential (11) can be written in the form

$$L^P(V_{TI}) = L^P(V_T) + L^P(V_I). \quad (12)$$

So, by applying the traditional spherical approximation (Heiskanen and Moritz, 1967), we get the attraction of topographic and compensating masses:

$$A_{TI} = -\frac{\partial}{\partial r_p} V_{TI} = -\frac{\partial}{\partial r_p} V_T - \frac{\partial}{\partial r_p} V_I = A_T + A_I, \quad (13)$$

which is nothing else but the effect of the potential (11) into gravity disturbances:

$$\delta g_{TI}(P) = A_{TI}(P). \quad (14)$$

In similar way we get the effects of the potential (11) into gravity anomalies

$$\Delta g_{TI}(P) = -\frac{\partial V_{TI}(P)}{\partial r_p} - \frac{2V_{TI}(P)}{r_p} = \delta g_{TI}(P) - \frac{2V_{TI}(P)}{r_p}, \quad (15)$$

and into geoid heights as well:

$$\delta N_{II}(P) = \frac{V_{II}(P)}{\gamma_P}, \quad (16)$$

where  $\gamma_P$  is normal gravity at the point  $P$ .

By analogy with the traditional disturbing potential  $T$ , we must require that zero-degree harmonic is absent in the potential (11). This requirement is achieved if the sum of topographic and compensating masses is equal to zero. As a result, we come to the condition

$$\int_0^{2\pi} \int_0^\pi \left( \int_{r_1}^{r_2} \rho_c r^2 dr + \int_{t_1}^{t_2} \Delta \rho r^2 dr \right) \sin \vartheta d\vartheta d\lambda = 0, \quad (17)$$

which must be taken into account in computations of topographic-isostatic corrections.

### Spherical approximation of the topographic / isostatic potential

Now we will apply the next traditional assumptions:

- ◆ the figure of the geoid is the sphere of mean Earth's radius

$$r_1 = R = const; \quad (18)$$

- ◆ the topographic masses have constant density

$$\rho_c = const. \quad (19)$$

Also we will use the well-known Airy-Heiskanen model with local isostatic compensation (Moritz, 1990) that leads to next additional assumptions:

- ◆ the compensation masses have constant density, which is equal to density jump at the crust-mantle boundary (Moho boundary):

$$\Delta \rho = const; \quad (20)$$

- ◆ without the topographic and compensating masses, the (normal) Earth's crust have the (normal) thickness

$$D > 0, \quad (21)$$

and bounded by the geocentric radii

$$const = t_1 = R - D < R = r_1 = const. \quad (22)$$

We use these conditions for the deriving of the Moho boundary and the integration over geocentric distance. Next, more adequate conditions will be considered for the developing of the corresponding algorithm, which allows to use measured values of densities and Moho depths.

### Moho boundary from zero mass condition

With the above assumptions, the zero mass condition (17) may be expressed especially for the case of local compensation as

$$\rho_c \int_R^{r_2} r^2 dr + \Delta \rho \int_{R-D}^{t_2} r^2 dr = 0. \quad (23)$$

Considering (23) as a third degree equation regarding  $t_2$ , we get

$$t_2 = \sqrt[3]{(R-D)^3 - \frac{\rho_c}{\Delta \rho} (r_2^3 - R^3)}. \quad (24)$$

This expression gives the geocentric distance of Moho boundary, obtained in the frame of Airy-Heiskanen model in the spherical approximation. Note here, that by representing  $t_2$  and  $r_2$  in the forms

$$t_2 = R - D - d, \quad r_2 = R + h, \quad (25)$$

substituting (25) into (24) and applying Taylor linearization, we get the expression

$$d \approx \frac{\rho_c}{\Delta\rho} \left( \frac{R}{R-D} \right)^2 h, \quad (26)$$

which coincides exactly with that used in (Rummel et al., 1988; Tsoulis, 2001) for investigations of spectral properties of topographic / isostatic potential.

### Integration over geocentric distance

Next, we replace the integration over  $\mathcal{G}, \lambda$  by the integration over spherical distance  $\psi$  and azimuth  $\alpha$  in (4), (11). With the assumptions (18) – (22) the potentials become

$$V_T(P) = G\rho_c \int_0^{2\pi} \int_0^\pi \int_R^{r_2} \frac{r^2 \sin\psi}{l} dr d\psi d\alpha, \quad (27)$$

$$V_I(P) = G\Delta\rho \int_0^{2\pi} \int_0^\pi \int_{R-D}^{t_2} \frac{r^2 \sin\psi}{l} dr d\psi d\alpha. \quad (28)$$

After the integration over the variable  $r$ , we come to

$$V_T(P) = G\rho_c \frac{r_P^2}{2} \int_0^\pi \int_0^{2\pi} v|_R^{r_2} d\alpha d\psi, \quad (29)$$

$$V_I(P) = G\Delta\rho \frac{r_P^2}{2} \int_0^\pi \int_0^{2\pi} v|_{R-D}^{t_2} d\alpha d\psi, \quad (30)$$

where

$$v = v(x, \psi) = \left\{ \ell(x + 3\cos\psi) + (3\cos^2\psi - 1)\ln(\ell + x - \cos\psi) \right\} \sin\psi, \quad (31)$$

$$\ell = \frac{l}{r_P} = \sqrt{1 + x^2 - 2x\cos\psi}, \quad (32)$$

$$x = \frac{r}{r_P}. \quad (33)$$

The function (31) has no any singularity within the interval  $\psi \in [0, \pi]$ . With  $x \neq 1$  it follows immediately from (31):

$$v(x, 0) = v(x, \pi) = 0. \quad (34)$$

In the case  $x = 1$  the function (31) gives

$$v(1, \psi) = \left\{ (3\cos^2\psi - 1) \ln \left( 2\sin\frac{\psi}{2} + 2\sin^2\frac{\psi}{2} \right) + 2(3\cos\psi + 1) \sin\frac{\psi}{2} \right\} \sin\psi, \quad (35)$$

and, therefore

$$v(1, \pi) = 0, \quad (36)$$

$$v(1, 0) = \lim_{\psi \rightarrow 0} v(1, \psi) = 0. \quad (37)$$

By differentiating (29), (30) with respect to  $r_P$ , we get in accordance with (13):

$$A_T(P) = G\rho_c r_P \int_0^\pi \int_0^{2\pi} a|_R^{r_2} d\alpha d\psi, \quad (38)$$

$$A_I(P) = G\Delta\rho r_P \int_0^\pi \int_0^{2\pi} a|_{R-D}^{l_2} d\alpha d\psi, \quad (39)$$

where

$$a = a(x, \psi) = \frac{x^3}{\ell} \sin \psi - v(x, \psi). \quad (40)$$

Again, the function (40) has no singularity within the interval  $\psi \in [0, \pi]$ . With  $x \neq 1$  we get directly:

$$a(x, 0) = a(x, \pi) = 0. \quad (41)$$

With  $x = 1$  the function (40) transforms to

$$a(1, \psi) = \cos \frac{\psi}{2} - v(1, \psi), \quad (42)$$

and taking into account (36) and (37) we see that

$$a(1, \pi) = 0, \quad (43)$$

$$a(1, 0) = 1. \quad (44)$$

As a result, we see that the function (40) has the jump at  $(x = 1, \psi = 0)$ . The functions (31) and (40) are shown in the Figure 1. for  $x = 1$ .

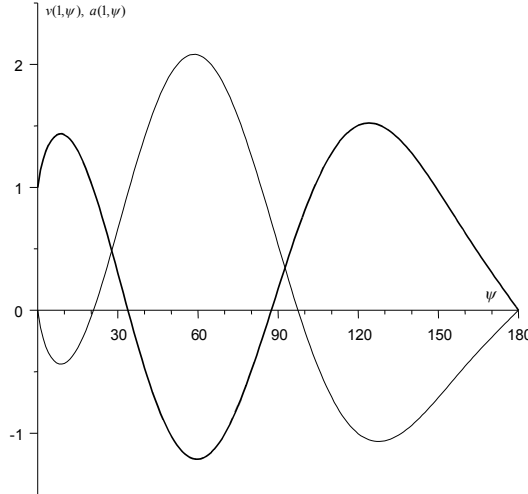


Fig. 1. Functions  $v(1, \psi)$  (simple curve) and  $a(1, \psi)$  (bold curve).

### Integration over spherical template compartments

Now we divide the spherical Earth's surface onto blocks in such a way that the geocentric distance (3) of the Earth's physical surface and the densities  $\rho_c, \Delta\rho$  may be taken as a constant within each block. If  $k$ -th block is bounded by the azimuths  $\alpha_1, \alpha_2$  and the spherical distances  $\psi_1, \psi_2$ , we can write

$$\rho_c(\psi, \alpha) = const, \quad r_2(\psi, \alpha) = const, \quad \psi \in [\psi_1, \psi_2], \quad \alpha \in [\alpha_1, \alpha_2]. \quad (45)$$

Also we have from (24) and (45):

$$\Delta\rho(\psi, \alpha) = const, \quad t_2(\psi, \alpha) = const, \quad \psi \in [\psi_1, \psi_2], \quad \alpha \in [\alpha_1, \alpha_2]. \quad (46)$$

These assumptions allow performing the integration within a block in (29), (30), (38) and (39). As a result, the following expressions are valid for a block:

$$V_T^k(P) = G\rho_c \frac{r_P^2}{2} \Delta\alpha \cdot w \Big|_{\psi_1}^{\psi_2} \Big|_{\psi_1}^{\psi_2}, \quad (47)$$

$$V_I^k(P) = G\Delta\rho \frac{r_P^2}{2} \Delta\alpha \cdot w \Big|_{R-D}^{\psi_2} \Big|_{\psi_1}^{\psi_2}, \quad (48)$$

$$A_T^k(P) = G\rho_c r_P \Delta\alpha \cdot b \Big|_{\psi_1}^{\psi_2} \Big|_{\psi_1}^{\psi_2}, \quad (49)$$

$$A_I^k(P) = G\Delta\rho \cdot r_P \Delta\alpha \cdot b \Big|_{R-D}^{\psi_2} \Big|_{\psi_1}^{\psi_2}. \quad (50)$$

In these formulas

$$\Delta\alpha = \alpha_2 - \alpha_1, \quad (51)$$

$$w = w(x, \psi) = \ell \left\{ \frac{2}{3} \ell^2 + (x - \cos \psi) \cos \psi \right\} + \sin^2 \psi \cos \psi \ln(\ell + x - \cos \psi), \quad (52)$$

$$b = b(x, \psi) = \ell x^2 - w(x, \psi), \quad (53)$$

and the quantities  $x$  and  $\ell$  are defined by the expressions (32), (33) respectively.

The functions (52), (53) have not a singularity at  $\psi = 0$  :

$$w(x, 0) = \lim_{\psi \rightarrow 0} w(x, \psi) = \frac{1}{3} |x-1| (x-1)(2x+1), \quad (54)$$

$$b(x, 0) = \lim_{\psi \rightarrow 0} b(x, \psi) = \frac{1}{3} |x-1| (x^2 + x + 1). \quad (55)$$

Moreover, these functions have non-singular first order derivatives with respect to  $\psi$ :

$$\frac{\partial w(x, \psi)}{\partial \psi} \Big|_{\psi=0} = \frac{\partial b(x, \psi)}{\partial \psi} \Big|_{\psi=0} = 0. \quad (56)$$

Figure 2 shows the functions (52), (53) with  $x = 1$  .

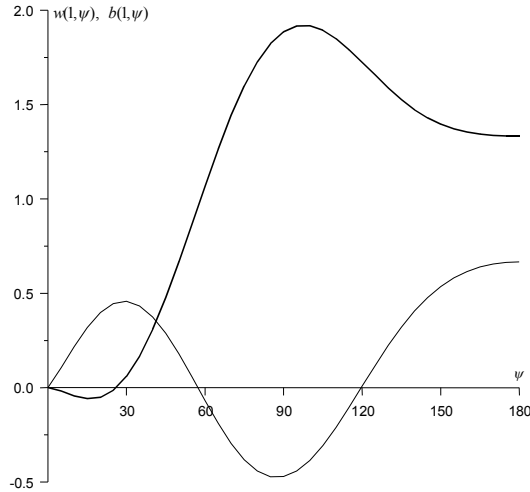


Fig. 2. Functions  $w(1, \psi)$  (simple curve) and  $b(1, \psi)$  (bold curve).

As a result, we can get potentials of topographic and compensating masses as well as corresponding attractions by the summation over all compartments

$$V_T(P) = \sum_k V_T^k(P), \quad (57)$$

$$V_I(P) = \sum_k V_I^k(P), \quad (58)$$

$$A_T(P) = \sum_k A_T^k(P), \quad (59)$$

$$A_I(P) = \sum_k A_I^k(P). \quad (60)$$

Derived expressions realize application of spherical mathematical template for computation of 3 dimensional integrals for topographic and isostatic potentials and corresponding attractions. In principle, such approach is well known in gravimetry and physical geodesy. For example, classical handbook by W.A.Heiskanen and H.Moritz (1967) contains detailed consideration of application of a mathematical template for computation of topographic / isostatic corrections in plane approximation.

### Conclusions

Both above considered approaches to computation of topographic / isostatic corrections are based on application of mathematical templates (spherical or planar) constructed around a point of interest. Closed expressions for the potential and the attraction obtained for each compartment of a template provide good practical flexibility of the discussed technique. In fact, because the requirements on constant densities  $\rho_c$  and  $\Delta\rho$  are essential strictly just within a compartment, we see the possibility to use observed density data without any modifications of above derived expressions (47) – (50) or (82) – (85). Moreover, seismically observed Moho depth data can be used also within each compartment.

Using the ETOPO1 digital terrain model (Fig. 3 and 4) we get two sets of the terrain reductions, one based on topographic surface data, second one – on the combination of the ice shield data and topography (Fig. 3–6 see at the color paste between pages 112 and 113).

From the Fig. 5 we can really fill how big the differences between the ice shield and topography at the Antarctic continent.

As a result two sets of the Fay anomaly were calculated. In the next step on the frame of well-known remove-restore technic the EGM2008 global gravity model was removed from the resulted sets of Fay anomalies. Using the sequential multipole analysis the residual gravity field was approximated by the sets of multipoles of different degree and order. But this is a topic of another paper.

With gridded data we can provide simple and effective interpolation of corresponding values onto centers of a template compartments. Usually, regular height data are available in the form of digital terrain models (DTM) with various resolutions. Much probably that data of other types are not available as corresponding grids. In this case general prediction techniques should be applied to irregular data for a grid creation. Next, we should note that choice of a template steps over azimuth and spherical (or horizontal) distance seems as practically important problem.

Indeed, very small steps will produce essential computation time expenses whereas too large steps will violate the conditions (45), (46) or (80), (81). In this view we should note that template steps must be agreed with smallest size of used grids. In addition, it may be necessary to perform grid densification in small vicinity of a computation point. It is obvious that application of the spherical template lead to more consistent results.

Finally, we should note that some modification of classical mathematical template was proposed by R.Forsberg (1984), who used division onto rectangular blocks in accordance with

DTM structure. However, potentials of rectangular prism were derived in (Forsberg, 1984) only as plane approximations of the potentials (4), (9). In addition, singularities may appear for some positions of computation point regarding DTM nodes. With this respect we can conclude that the technique based on rectangular prism potentials has not essential advantages in comparison with the techniques based on classical mathematical templates.

### References

**Forsberg, R.** (1984) A study of terrain reductions, density anomalies and geophysical inversion methods in gravity field modeling. Reports of the Department of Geodetic Science and Surveying, Ohio State University, Report No. 355.

**Heiskanen, W.A., and Moritz, H.** (1967) Physical Geodesy. W.H. Freeman, San Francisco.

**Moritz, H.** (1980) Advanced Physical Geodesy, H. Wichmann, Karlsruhe, 1980.

**Moritz, H.** (1990) The Figure of the Earth. Theoretical Geodesy and Earth's Interior, Wichmann, Karlsruhe, 1990.

**Neyman, Yu.M.** (1979) Variational Method of Physical Geodesy. Nedra: Moscow. (In Russian).

**Rummel, R., Rapp, R.H., Sünkel, H., Tscherning, C.C.** (1988) Comparisons of global topographic / isostatic models to the Earth's observed gravity field. Reports of the Department of Geodetic Science and Surveying, Ohio State University, Report No. 388.

**Tsoulis, D.** (2001) A comparison between the Airy/Heiskanen and the Pratt/Hayford isostatic models for the computation of potential harmonic coefficients // *Journal of Geodesy*, No. 74, p. 637–643.

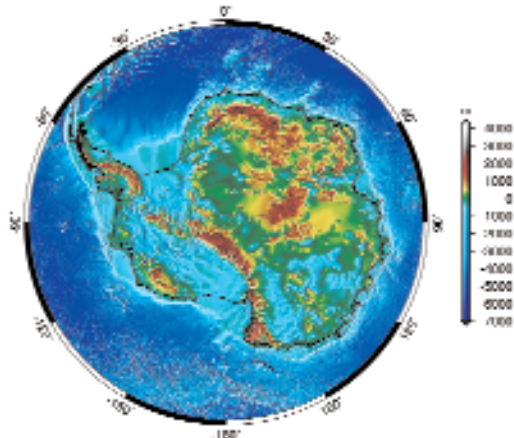


Fig. 3. ETOPO 1 terrain surface

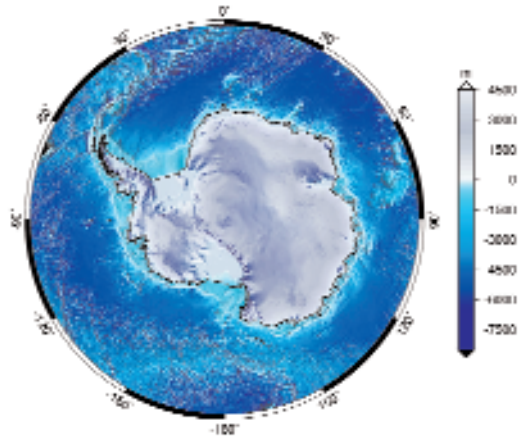


Fig. 4. ETOPO 1 ice surface

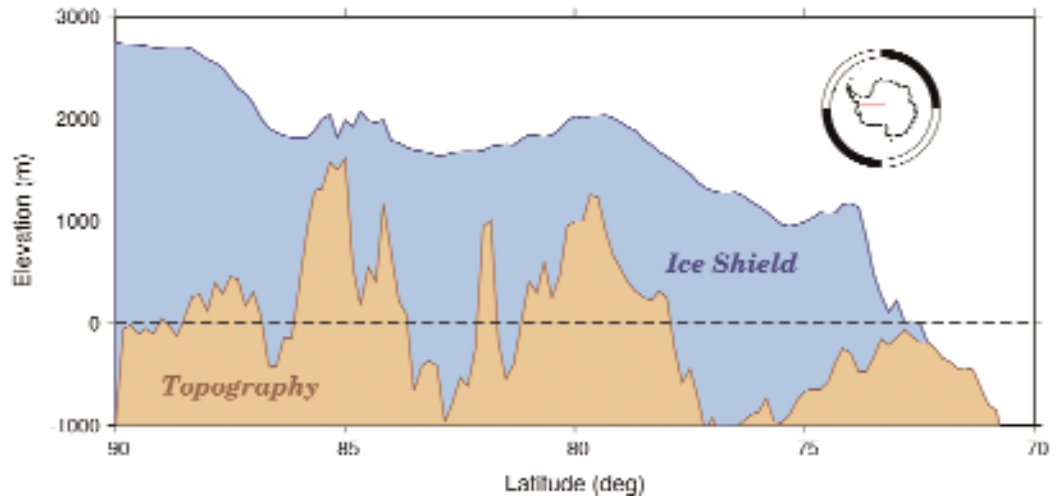


Fig. 5. Ice surface and topography along the track limited by 90S to 70S and 90W

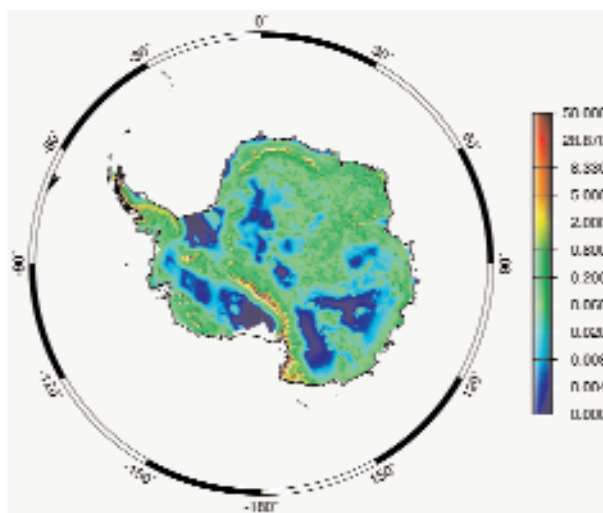


Fig. 6. Terrain correction based on combination of ice surface and topography data (mGal)